Reactor measurement of θ13 and its complementarity to long-baseline experiments

doi: 10.1103/PhysRevD.68.033017

Reactor measurement of θ_{13} and its complementarity to long-baseline experiments

H. Minakata,* H. Sugiyama,† and O. Yasuda‡
Department of Physics, Tokyo Metropolitan University, Hachioji, Tokyo 192-0397, Japan

K. Inoue§ and F. Suekane‖
Research Center for Neutrino Science, Tohoku University, Sendai, Miyagi, 980-8578, Japan

(Received 8 November 2002; revised manuscript received 18 April 2003; published 28 August 2003)

The possibility of measuring $\sin^2 2\theta_{13}$ using reactor neutrinos is examined in detail. It is shown that the sensitivity $\sin^2 2\theta_{13} > 0.02$ can be reached with 40 ton yr data by placing identical CHOOZ-like detectors at near and far distances from a giant nuclear power plant whose total thermal energy is 24.3 GW_{th}. It is emphasized that this measurement is free from the parameter degeneracies that occur in accelerator appearance experiments, and therefore the reactor measurement is complementary to accelerator experiments. It is also shown that the reactor measurement may be able to resolve the degeneracy in θ_{23} if $\sin^2 2\theta_{13}$ and $\cos^2 2\theta_{23}$ are relatively large.

DOI: 10.1103/PhysRevD.68.033017 PACS number(s): 14.60.Pq, 25.30.Pt, 28.41.−i

I. INTRODUCTION

Despite the accumulating knowledge of neutrino masses and lepton flavor mixing from atmospheric [1], solar [2,3], and accelerator [4] neutrino experiments, the (1-3) sector of the Maki-Nakagawa-Sakata (MNS) matrix [5] is still unclear. At the moment, we know only that $|U_{e3}| = \sin\theta_{13} \equiv s_{13}$ is small, $s^2_{13} \lesssim 0.03$, from the bound imposed by the CHOOZ reactor experiment [6]. In this paper we assume that the light neutrino sector consists of three active neutrinos only. One of the challenging goals in the attempt to explore the full structure of lepton flavor mixing would be measuring the leptonic *CP* or *T* violating phase δ in the MNS matrix. If the KamLAND experiment [7] confirms the large-mixing-angle (LMA) Mikheyev-Smirnov-Wolfenstein (MSW) [8,9] solution of the solar neutrino problem, the one most favored by recent analyses of solar neutrino data [3,10], we will have an open route toward this goal. Yet there might still exist a last impasse, namely, the possibility of a too small value of θ_{13}. Thus, it has recently been emphasized more and more strongly that the crucial next step toward the goal is the determination of θ_{13}.

In this paper, we raise the possibility that a $\overline{\nu}_e$ disappearance experiment using reactor neutrinos could be potentially the fastest (and the cheapest) way to detect the effects of a nonzero θ_{13}. In fact, such an experiment using the Krasnoyarsk reactor complex was described earlier [11], in which the sensitivity to $\sin^2 2\theta_{13}$ can be as low as ~ 0.01, an order of magnitude lower than in the CHOOZ experiment. We also briefly outline basic features of our proposal and reexamine the sensitivity to $\sin^2 2\theta_{13}$ in this paper.

It appears that the most popular way of measuring θ_{13} is the next generation long-baseline (LBL) neutrino oscillation experiments MINOS [12], OPERA [13], and JHF phase I [14]. It may be followed either by conventional superbeam [15] experiments (the JHF phase II [14] and possibly others [16,17]) or by experiments at neutrino factories [18,19]. It is pointed out, however, that the measurement of θ_{13} in LBL experiments with only a neutrino channel (as planned in JHF phase I) would suffer from large intrinsic uncertainties, on top of the experimental errors, due to the dependence on an unknown *CP* phase and the sign of Δm^2_{31} [20]. Furthermore, it is noticed that an ambiguity remains in the determination of θ_{13} and other parameters even if precise measurements of the appearance probabilities in neutrino as well as antineutrino channels are carried out, that is, the problem of the parameter degeneracy [20–26]. (For a global overview of parameter degeneracy, see [26].) While some ideas toward a solution have been proposed, the problem is hard to solve experimentally, and it is not likely to be resolved in the near future.

We emphasize in this paper that reactor $\overline{\nu}_e$ disappearance experiments provide a particularly clean environment for the measurement of θ_{13}; namely, it can be regarded as a dedicated experiment for determination of θ_{13}; it is insensitive to the ambiguity due to all the remaining oscillation parameters as well as to the matter effect. This is in sharp contrast with the features of LBL experiments described above. Thus, the reactor measurement of θ_{13} will provide us with valuable information complementary to that from LBL experiments and will play an important role in resolving the problem of parameter degeneracy. We show here that reducing the systematic errors is crucial for the reactor measurement of θ_{13} to be competitive in accuracy with LBL experiments. We present a preliminary analysis of its possible role in this context. It is then natural to think about the possibility that one has better control by combining the two complementary way of measuring θ_{13}, the reactor and the accelerator methods. In fact, we show in this paper that nontrivial relations exist between the θ_{13} measurements by the two methods thanks to their complementary nature, so that in the luckiest case one may be able to derive constraints on the value of the *CP* violating phase δ or determine the neutrino mass hierarchy.

*Electronic address: minakata@phys.metro-u.ac.jp
†Electronic address: hiroaki@phys.metro-u.ac.jp
‡Electronic address: yasuda@phys.metro-u.ac.jp
§Electronic address: inoue@awa.tohoku.ac.jp
‖Electronic address: suekane@awa.tohoku.ac.jp

II. REACTOR EXPERIMENT AS A CLEAN LABORATORY FOR θ_{13} MEASUREMENT

Let us examine in this section how clean the measurement of θ_{13} by a reactor experiments is. To define our notation, we note that the standard notation [27]

$$U=\begin{bmatrix} c_{12}c_{13} & s_{12}c_{13} & s_{13}e^{-i\delta} \\ -s_{12}c_{23}-c_{12}s_{23}s_{13}e^{i\delta} & c_{12}c_{23}-s_{12}s_{23}s_{13}e^{i\delta} & s_{23}c_{13} \\ s_{12}s_{23}-c_{12}c_{23}s_{13}e^{i\delta} & -c_{12}s_{23}-s_{12}c_{23}s_{13}e^{i\delta} & c_{23}c_{13} \end{bmatrix} \tag{1}$$

is used for the MNS matrix throughout this paper, where c_{ij} and s_{ij} $(i,j=1-3)$ imply $\cos\theta_{ij}$ and $\sin\theta_{ij}$, respectively. The mass squared difference of the neutrinos is defined as $\Delta m^2_{ij}\equiv m^2_i-m^2_j$, where m_i is the mass of the ith eigenstate.

We examine possible "contamination" by δ, the matter effect, the sign of Δm^2_{31}, and the solar parameters one by one. We first note that, due to the low neutrino energy of a few MeV, reactor experiments are inherently disappearance experiments, which can measure only the survival probability $P(\overline{\nu}_e\to\overline{\nu}_e)$. It is well known that the survival probability does not depend on the *CP* phase δ in arbitrary matter densities [28].

In any reactor experiment on the Earth, short or long baseline, the matter effect is very small because the energy is quite low and can be ignored to a good approximation. This can be seen by comparing the matter and the vacuum effects (as the matter correction comes in only through this combination in the approximate formula in [18]):

$$\frac{aL}{|\Delta_{31}|}=2.8\times10^{-4}\left(\frac{|\Delta m^2_{31}|}{2.5\times10^{-3}\ \mathrm{eV}^2}\right)^{-1}\left(\frac{E}{4\ \mathrm{MeV}}\right)\times\left(\frac{\rho}{2.3\ \mathrm{g\,cm}^{-3}}\right)\left(\frac{Y_e}{0.5}\right), \tag{2}$$

where

$$\Delta_{ij}\equiv\frac{\Delta m^2_{ij}L}{2E} \tag{3}$$

with E being the neutrino energy and L the baseline length. The best fit value of $|\Delta m^2_{31}|$ is given by $|\Delta m^2_{31}|=2.5\times10^{-3}$ eV^2 from the Super-Kamiokande atmospheric neutrino data [29], and we use this as the reference value for $|\Delta m^2_{31}|$ throughout this paper. $a=\sqrt{2}G_FN_e$ denotes the index of refraction in matter with G_F being the Fermi constant and N_e the electron number density on Earth, which is related to the Earth matter density ρ as $N_e=Y_e\rho/m_p$ where Y_e is the proton fraction. Once we know that the matter effect is negligible we immediately recognize that the survival probability is independent of the sign of Δm^2_{31}.

Therefore, the vacuum probability formula applies. The general probability formula in vacuum is analytically written as [27]

$$\left.\begin{matrix}P(\nu_\alpha\to\nu_\beta)\\ P(\overline{\nu}_\alpha\to\overline{\nu}_\beta)\end{matrix}\right\}=\delta_{\alpha\beta}-4\sum_{j<k}\mathrm{Re}(U_{\alpha j}U^*_{\beta j}U^*_{\alpha k}U_{\beta k})\times\sin^2\left(\frac{\Delta m^2_{jk}L}{4E}\right)\mp2\sum_{j<k}\mathrm{Im}(U_{\alpha j}U^*_{\beta j}U^*_{\alpha k}U_{\beta k})\times\sin\left(\frac{\Delta m^2_{jk}L}{2E}\right), \tag{4}$$

where $\alpha,\beta=e,\mu,\tau$, and the minus and plus signs in front of the $\mathrm{Im}(U_{\alpha j}U^*_{\beta j}U^*_{\alpha k}U_{\beta k})$ term correspond to neutrino and antineutrino channels, respectively. From Eq. (4) the exact expression for $P(\overline{\nu}_e\to\overline{\nu}_e)$ is given by

$$\begin{aligned}1-P(\overline{\nu}_e\to\overline{\nu}_e)&=4\sum_{j<k}|U_{ej}|^2|U_{ek}|^2\sin^2\left(\frac{\Delta m^2_{jk}L}{4E}\right)\\&=\sin^2 2\theta_{13}\sin^2\frac{\Delta_{31}}{2}\\&\quad+\frac{1}{2}c^2_{12}\sin^2 2\theta_{13}\sin\Delta_{31}\sin\Delta_{21}\\&\quad+(c^4_{13}\sin^2 2\theta_{12}+c^2_{12}\sin^2 2\theta_{13}\cos\Delta_{31})\times\sin^2\frac{\Delta_{21}}{2},\end{aligned} \tag{5}$$

where the parametrization (1) has been used in the second equality. The last three terms in the second equality of Eq. (5) are suppressed relative to the main depletion term, the first term of the right-hand side of Eq. (5), by ϵ, $\epsilon^2/\sin^2 2\theta_{13}$, and ϵ^2, respectively, where $\epsilon\equiv\Delta m^2_{21}/|\Delta m^2_{31}|$. Assuming that $|\Delta m^2_{31}|=(1.6\text{–}3.9)\times10^{-3}$ eV^2 [29], $\epsilon\simeq0.1$–0.01 for the LMA MSW solar neutrino solution [3,10]. Then, the second and fourth terms in the second equality can be ignored, although the third term can be of order unity compared with the main depletion term provided that $\epsilon\simeq0.1$. (Notice that we are considering the measurement of $\sin^2 2\theta_{13}$ in the range of 0.1–0.01.) Therefore, assuming that $|\Delta m^2_{31}|$ is determined by LBL experiments with good accuracy, the reactor $\overline{\nu}_e$ disappearance experiment gives us a clean measurement of θ_{13} which is independent of any solar parameters except for the case of high Δm^2_{21} LMA solutions.

If the high Δm^2_{21} LMA solution with $\Delta m^2_{21}\sim10^{-4}$ eV^2 turns out to be the right one, we need to take special care of

TABLE I. Systematic errors in the Bugey and CHOOZ-like experiments. Relative errors in the CHOOZ-like experiment are those expected with the same reduction rates of errors as those of Bugey.

Bugey	Absolute normalization	Relative normalization	Relative/ absolute
Flux	2.8%	0.0%	0
Number of protons	1.9%	0.6%	0.32
Solid angle	0.5%	0.5%	1
Detection efficiency	3.5%	1.7%	0.49
Total	4.9%	2.0%	

CHOOZ-like	Absolute normalization	Relative normalization (expected)	Relative/ absolute
Flux	2.1%	0.0%	0
Number of protons	0.8%	0.3%	0.38
Detection efficiency	1.5%	0.7%	0.47
Total	2.7%	0.8%	
For bins	8.1%	2.4%	

the second term of the second equality of Eq. (5). In this case, the determination of θ_{13} and the solar angle θ_{12} are inherently coupled,[1] and we would need a joint analysis from a near-far detector complex (see the next section) and KamLAND.

III. NEAR-FAR DETECTOR COMPLEX: BASIC CONCEPTS AND ESTIMATION OF SENSITIVITY

In order to obtain good sensitivity to $\sin^2 2\theta_{13}$, the selection of an optimized baseline and having small statistical and systematic errors are crucial. For instance, the baseline length that gives the oscillation maximum for reactor $\bar{\nu}_e$'s which have typical energy 4 MeV is 1.7 km for $\Delta m^2 \simeq 2.5 \times 10^{-3}$ eV^2. Along with this baseline selection, if systematic and statistical errors can be reduced to the 1% level, which is 2.8 times better than the CHOOZ experiment [6], an order of magnitude improvement for the $\sin^2 2\theta_{13}$ sensitivity is possible at $\Delta m^2 \simeq 2.5 \times 10^{-3}$ eV^2. In this section we demonstrate that this kind of experiment is potentially possible if we place a CHOOZ-like detector with a baseline of 1.7 km 200 m underground near a reactor of 24.3 GW$_{\rm th}$ thermal power. The reactor can be regarded as a simplified version of the Kashiwazaki-Kariwa nuclear power plant, which consists of seven reactors whose maximum energy generation is 24.3 GW$_{\rm th}$.

The major part of the systematic error is caused by uncertainties in the neutrino flux calculation, the number of protons, and the detection efficiency. For instance, in the CHOOZ experiment, the uncertainty of the neutrino flux is 2.1%, that of the number of protons is 0.8%, and that of the detection efficiency 1.5%, as is shown in Table I. The uncertainty of the neutrino flux includes ambiguities of the reactor thermal power generation, the reactor fuel component, the neutrino spectra from fission, and so on. The uncertainty of the detection efficiency includes a systematic shift in defining the fiducial volume. These systematic uncertainties, however, cancel out if identical detectors are placed near and far from the reactors and data taken at the different detectors are compared.[2]

To estimate how good the cancellation will be, we study the case of the Bugey experiment, which uses three identical detectors to detect reactor neutrinos at 14, 40, and 90 m. For the Bugey case, the uncertainty of the neutrino flux improved from 3.5% to 1.7% and the error on the solid angle remained the same (0.5%→0.5%). If each ratio of the improvement for the Bugey case is directly applicable to our case, the systematic uncertainty will improve from 2.7% to 0.8% as shown in Table I. The ambiguity in the solid angle will be negligibly small because the absolute baseline is much longer than in the Bugey case. We are thinking of the case where the front detector is located 300 m away from the

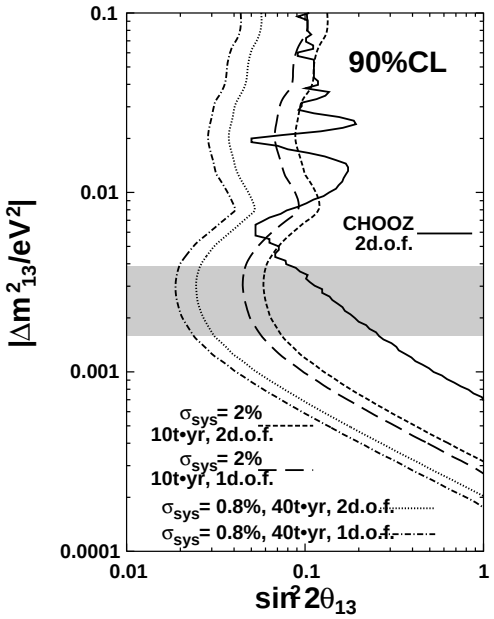

FIG. 1. Shown are the 90% C.L. exclusion limits on $\sin^2 2\theta_{13}$ that can be placed by the reactor measurement as described in Sec. III. From left to right, the dash-dotted and dotted (the long-dashed and short-dashed) lines are based on analyses with one and two degrees of freedom (see the text), respectively, for $\sigma_{\rm sys}=0.8\%$, 40 ton yr ($\sigma_{\rm sys}=2\%$, 10 ton yr). The solid line is the CHOOZ result, and the 90% C.L. interval 1.6×10^{-3} eV$^2 \leqslant \Delta m^2_{31} \leqslant 3.9\times10^{-3}$ eV^2 of the Super-Kamiokande atmospheric neutrino data is shown as a shaded strip.

[1]The effect of nonzero θ_{13} for measurement of θ_{12} at KamLAND is discussed in [30].

[2]This is more or less the strategy taken in the Bugey experiment [31]. The Krasnoyarsk group also plans in their Kr2Det proposal [11] to construct two identical 50 ton liquid scintillators at 1100 m and 150 m from the Krasnoyarsk reactor. They indicate that the systematic error can be reduced to 0.5% by comparing the near and far detectors.

reactor we consider. In the actual setting with the Kashiwazaki-Kariwa power plant, two near detectors may be necessary due to the extended array of seven reactors. Hereafter, we take 2% and 0.8% as the reference values for the relative systematic error $\sigma_{\rm sys}$ for the total number of $\bar{\nu}_e$ events in our analysis. Let us examine the physics potential of such a reactor experiment, assuming these reference values for the systematic error. We take, for concreteness, the Kashiwazaki-Kariwa reactor of 24.3 $GW_{\rm th}$ thermal power and assume its operation with 80% efficiency. Two identical liquid scintillation detectors are located at 300 m and 1.7 km away from the reactor and assumed to detect $\bar{\nu}_e$ by delayed coincidence with 70% detection efficiency. $\bar{\nu}_e$'s of 1–8 MeV visible energy, $E_{\rm visi}=E_{\bar{\nu}_e}-0.8$ MeV, are used and the number of events is counted in 14 bins of 0.5 MeV. Without oscillation, a 10 (40) ton yr measurement at the far detector yields 20 000 (80 000) $\bar{\nu}_e$ events, which is naively comparable to a 0.7% (0.35%) statistical error.

First, let us calculate how much we could constrain $\sin^2 2\theta_{13}$. Unlike the analysis in [31], which uses the ratio of the numbers of events at the near and far detectors, we use the difference of the numbers of events $N_i(L_2)-(L_1/L_2)^2 N_i(L_1)$, because statistical analysis with ratios is complicated (see, e.g., [32]). The definition of $\Delta\chi^2$, which stands for the deviation from the best fit point (nonoscillation point), is given by

$$\Delta\chi^2(\sin^2 2\theta_{13},|\Delta m^2_{31}|)\equiv\sum_{i=1}^{14}\frac{\{[N_{i(0)}(L_2)-(L_1/L_2)^2N_{i(0)}(L_1)]-[N_i(L_2)-(L_1/L_2)^2N_i(L_1)]\}^2}{N_{i(0)}(L_2)+(L_1/L_2)^4N_{i(0)}(L_1)+(\sigma^{\rm bin}_{\rm sys})^2N^2_{i(0)}(L_2)},\tag{6}$$

$$N_i(L_j)\equiv N_i(\sin^2 2\theta_{13},|\Delta m^2_{31}|;L_j),\quad N_{i(0)}(L_j)\equiv N_i(0,0;L_j),$$

where $\sigma^{\rm bin}_{\rm sys}$ is the relative systematic error for each bin, which is assumed to be the same for all bins, and $N_i(\sin^2 2\theta_{13},|\Delta m^2_{31}|)$ denotes the theoretical number of $\bar{\nu}_e$ events within the ith energy bin. In principle both the systematic errors $\sigma^{\rm bin}_{\rm abs\ sys}$ (absolute normalization) and $\sigma^{\rm bin}_{\rm sys}$ (relative normalization) appear in the denominator of Eq. (6), but by taking the difference, we have $(1+\sigma^{\rm bin}_{\rm abs\ sys})[(1+\sigma^{\rm bin}_{\rm sys})N_i(L_2)-(L_1/L_2)^2N_i(L_1)]-[N_i(L_2)-(L_1/L_2)^2N_i(L_1)]=\sigma^{\rm bin}_{\rm sys}N_i(L_2)+\sigma^{\rm bin}_{\rm abs\ sys}[N_i(L_2)-(L_1/L_2)^2N_i(L_1)]$, which indicates that the systematic error is dominated by the relative error $\sigma^{\rm bin}_{\rm sys}$, as the second term $[N_i(L_2)-(L_1/L_2)^2N_i(L_1)]$ is supposed to be small. In fact we have explicitly verified numerically that the presence of $(\sigma^{\rm bin}_{\rm abs\ sys})^2[N_i(L_2)-(L_1/L_2)^2N_i(L_1)]^2$ in the denominator of Eq. (6) does not affect any of our results. From the assumption that the relative systematic error for each bin is distributed equally into the bins, $\sigma^{\rm bin}_{\rm sys}$ is estimated from the relative systematic error $\sigma_{\rm sys}$ for the total number of events by

$$(\sigma^{\rm bin}_{\rm sys})^2=\sigma^2_{\rm sys}\frac{[N^{\rm tot}_{(0)}(L_2)]^2}{\sum_i N^2_{i(0)}(L_2)},\quad N^{\rm tot}_{(0)}(L_2)\equiv\sum_i N_{i(0)}(L_2),\tag{7}$$

since the uncertainty squared of the total number of events is obtained by adding up the bin-by-bin systematic errors $(\sigma^{\rm bin}_{\rm sys})^2N^2_{i(0)}(L_2)$; the ratio $\sigma^{\rm bin}_{\rm sys}/\sigma_{\rm sys}$ is about 3 in our analysis. In Fig. 1, the 90% C.L. exclusion limits, which correspond to $\Delta\chi^2=2.7$ for one degree of freedom (DOF), are presented for two cases: a 10 ton yr measurement with 2% systematic error of the total number of events and a 40 ton yr measurement with 0.8% error. The figure shows that it is possible to measure $\sin^2 2\theta_{13}$ down to 0.02 at the maximum sensitivity with respect to $|\Delta m^2_{31}|$, and to 0.04 for larger $|\Delta m^2_{31}|$, by a 40 ton yr measurement, provided the quoted values of the systematic errors are realized. The CHOOZ result [6] is also depicted in Fig. 1. For a fair comparison with the CHOOZ contour, we also present in Fig. 1 the results of an analysis with two degrees of freedom, which correspond to $\Delta\chi^2=4.6$ for 90% C.L., without assuming any precise knowledge of $|\Delta m^2_{31}|$.

Next, let us examine how precisely we could measure $\sin^2 2\theta_{13}$. The definition of $\Delta\chi^2$ is

$$\Delta\chi^2(\sin^2 2\theta_{13},|\Delta m^2_{31}|)\equiv\sum_{i=1}^{14}\frac{\{[N_{i(\rm best)}(L_2)-(L_1/L_2)^2N_{i(\rm best)}(L_1)]-[N_i(L_2)-(L_1/L_2)^2N_i(L_1)]\}^2}{N_{i(\rm best)}(L_2)+(L_1/L_2)^4N_{i(\rm best)}(L_1)+(\sigma^{\rm bin}_{\rm sys})^2N^2_{i(\rm best)}(L_2)},\tag{8}$$

where $N_{i(\rm best)}$ denotes N_i for the set of best fit parameters $(\sin^2 2\theta^{(\rm best)}_{13},|\Delta m^{2(\rm best)}_{31}|)$ given artificially. $\sigma^{\rm bin}_{\rm sys}$ is obtained in Eq. (7) by replacing $N_{i(0)}$ with $N_{i(\rm best)}$ and the ratio $\sigma^{\rm bin}_{\rm sys}/\sigma_{\rm sys}$ is about 3 again. We assume that the value of $|\Delta m^2_{31}|$ is known to a precision of 10^{-4} eV^2 from JHF phase I by the time the reactor measurement is actually utilized to solve the degeneracy. Then we rely on the analysis with one degree of freedom, fixing $|\Delta m^2_{31}|$ as $|\Delta m^{2(\rm best)}_{31}|=2.5\times10^{-3}$ eV^2. The

90% C.L. allowed regions for one degree of freedom, whose bounds correspond to $\Delta\chi^2=2.7$, are presented in Fig. 2 for the values of $\sin^2 2\theta_{13}^{(\mathrm{best})}$ from 0.05 to 0.08 (0.02 to 0.08) in units of 0.01 in the case of a 10 ton yr (40 ton yr) measurement with systematic error $\sigma_{\mathrm{sys}}=2.0\%$ (0.8%). We can read off the error at 90% C.L. in $\sin^2 2\theta_{13}$ and it is almost independent of the central value $\sin^2 2\theta_{13}^{(\mathrm{best})}$. Thus, we have

$$\sin^2 2\theta_{13}=\sin^2 2\theta_{13}^{(\mathrm{best})}\pm 0.043$$

$$(\text{at 90\% C.L., DOF}=1)\ \text{for}\ \sin^2 2\theta_{13}^{(\mathrm{best})}\gtrsim 0.05$$

in the case of $\sigma_{\mathrm{sys}}=2\%$ with a 10 ton yr measurement, and

$$\sin^2 2\theta_{13}=\sin^2 2\theta_{13}^{(\mathrm{best})}\pm 0.018$$

$$(\text{at 90\% C.L., DOF}=1)\ \text{for}\ \sin^2 2\theta_{13}^{(\mathrm{best})}\gtrsim 0.02$$

in the case of $\sigma_{\mathrm{sys}}=0.8\%$ with a 40 ton yr measurement.

IV. THE PROBLEM OF THE $(\theta_{13},\delta,\theta_{23},\Delta m^2_{31})$ PARAMETER DEGENERACY

We explore in this and the following sections the possible significance of reactor measurements of θ_{13} in the context of the problem of parameter degeneracy. We show that a reactor measurement of θ_{13} can resolve the degeneracy at least partly if the measurement is sufficiently accurate. Toward this goal, we first explain the problem of parameter degeneracy in long-baseline neutrino oscillation experiments. It is a notorious problem; a set of measurements of the ν_μ disappearance probability and the appearance oscillation probabilities of $\nu_\mu\to\nu_e$ and $\bar{\nu}_\mu\to\bar{\nu}_e$, no matter how accurate they may be, does not allow unique determination of θ_{13}, δ, and θ_{23}. The problem was first recognized in the form of intrinsic degeneracy between the two sets of solutions of $(\theta_{23},\theta_{13})$ for a given set of measurements in two different channels $\nu_\mu\to\nu_e$ and $\nu_\mu\to\nu_\tau$ [21]. It was then observed independently that a similar degeneracy of solutions of (θ_{13},δ) exists in measurements of ν_e appearance in the neutrino and antineutrino channels [22]. The authors of [22] made the first systematic analysis of the degeneracy problem. It was noticed that the degeneracy is further duplicated provided that two neutrino mass patterns, the normal $(\Delta m^2_{31}>0)$ and the inverted $(\Delta m^2_{31}<0)$ hierarchies, are allowed [23]. Finally, it was pointed out that the degeneracy can be maximally eightfold [24]. The analytical structure of the degenerate solutions was worked out in a general setting in [26].

To illuminate the point, let us first restrict our treatment to a relatively short-baseline experiment such as the CERN Frejus project [16]. In this case, one can use the vacuum oscillation approximation for the disappearance and appearance probabilities. From the general formula (4) we have

$$1-P(\nu_\mu\to\nu_\mu)=4\sum_{j<k}|U_{\mu j}|^2|U_{\mu k}|^2\sin^2\left(\frac{\Delta m^2_{jk}L}{4E}\right)$$

$$=\sin^2 2\theta_{23}\sin^2\frac{\Delta_{31}}{2}-\left(\frac{1}{2}c_{12}^2\sin^2 2\theta_{23}-s_{13}s_{23}^2\sin 2\theta_{23}\sin 2\theta_{12}\cos\delta\right)\sin\Delta_{21}\sin\Delta_{31}+O(\epsilon^2)+O(s_{13}^2),\quad(9)$$

$$\left.\begin{matrix}P(\nu_\mu\to\nu_e)\\ P(\bar{\nu}_\mu\to\bar{\nu}_e)\end{matrix}\right\}=-4\sum_{j<k}\mathrm{Re}(U_{\mu j}U_{ej}^*U_{\mu k}^*U_{ek})\sin^2\left(\frac{\Delta m^2_{jk}L}{4E}\right)\mp 2\sum_{j<k}\mathrm{Im}(U_{\mu j}U_{ej}^*U_{\mu k}^*U_{ek})\sin\left(\frac{\Delta m^2_{jk}L}{2E}\right),$$

$$=s_{23}^2\sin^2 2\theta_{13}\sin^2\frac{\Delta_{31}}{2}+\frac{1}{2}J_r\sin\Delta_{21}\sin\Delta_{31}\cos\delta\mp J_r\sin\Delta_{21}\sin^2\frac{\Delta_{31}}{2}\sin\delta+O(\epsilon s_{13}^2),\quad(10)$$

where $\epsilon\equiv\Delta m^2_{21}/|\Delta m^2_{31}|$, $J_r\equiv\sin 2\theta_{23}\sin 2\theta_{12}c_{13}^2 s_{13}$, and the parametrization (1) has been used in the second equality in each formula. The minus and plus signs in front of the $\sin\delta$ term in Eq. (10) correspond to the neutrino and antineutrino channels, respectively. The explicit perturbative computation in [33] indicates that the matter effect enters into the expression in a particular combination with other quantities (in the form of $s_{13}^2 aL/\Delta_{31}$), so that the effect is small. By the disappearance measurement at JHF, for example, $\sin^2 2\theta_{23}$ and $|\Delta m^2_{31}|$ will be determined with accuracies of 1% for 0.92

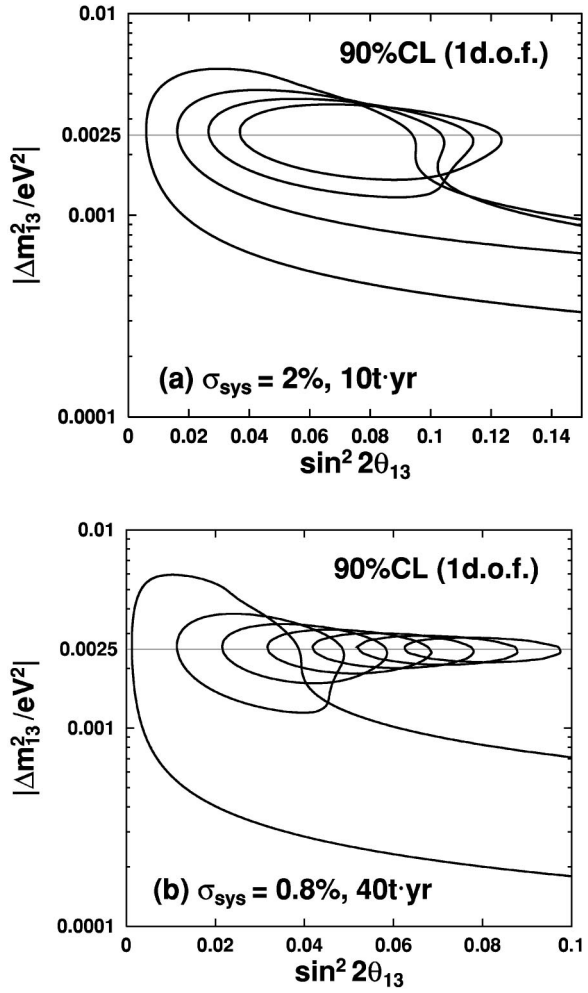

FIG. 2. Shown is the accuracy of determination of $\sin^2 2\theta_{13}$ at 90% C.L. for the case of positive evidence based on analysis with one degree of freedom, $\Delta\chi^2=2.7$. Figures (a) and (b) are for $\sigma_{\rm sys}=2\%$, 10 ton yr, and $\sigma_{\rm sys}=0.8\%$, 40 ton yr, respectively. The lines correspond to the best fit values of $\sin^2 2\theta_{13}$, from left to right, 0.05 to 0.08 in units of 0.01 in (a), and 0.02 to 0.08 in units of 0.01 in (b). The reference value of $|\Delta m^{2(\rm best)}_{31}|$ is taken to be 2.5×10^{-3} eV^2, which is indicated by a gray line.

$\leqslant \sin^2 2\theta_{23} \leqslant 1.0$ (Fig. 11 in [14]) and 4%, respectively [14].[3] If θ_{23} is not maximal, then we have two solutions for θ_{23} (θ_{23} and $\pi/2-\theta_{23}$), even if we ignore the uncertainty in the determination of $\sin^2 2\theta_{23}$. For example, if $\sin^2 2\theta_{23}=0.95$, which is perfectly allowed by the most recent atmospheric neutrino data [29], then s^2_{23} can be either 0.39 or 0.61. Since the dominant term in the appearance probability depends upon s^2_{23} instead of $\sin^2 2\theta_{23}$, this leads to a $\pm 20\%$ difference in the number of appearance events in this case. On the other hand, in the case of maximal mixing, it still leaves a rather wide range of θ_{23}, despite the fantastic accuracy of the measurement. 1% accuracy in $\sin^2 2\theta_{23}$ implies about 10% uncertainty in s^2_{23}. Thus, whenever we try to determine $\sin^2 2\theta_{13}$ from the appearance measurement, we have to face the ambiguity due to the twofold nature of the solution for s^2_{23}.

Let us discuss the simplest possible case, the low Δm^2 or the vacuum oscillation solution of the solar neutrino problem. (See, e.g., [34] for a recent discussion.) In this case, one can safely ignore terms of order ϵ in Eqs. (9) and (10). Then we are left with only the first terms in the second equality of these equations, the one-mass-scale dominant vacuum oscillation probabilities. Now let us define the symbols $x=\sin^2 2\theta_{13}$ and $y=s^2_{23}$. Then, Eqs. (9) and (10) take the forms $y=y_1$ or y_2 (corresponding to two solutions of s^2_{23}) and $xy=$const, respectively, for given values of the probabilities. It is then obvious that there are two crossing points of these curves. This is the simplest version of the $(\theta_{13},\theta_{23})$ degeneracy problem. We next discuss what happens if ϵ is not negligible although small: the case of the LMA solar neutrino solution. In this case, the appearance curve $xy=$const is split into two curves (although they are in fact connected at their maximum value of s^2_{23}) because of the two degenerate solutions of the set (δ,θ_{13}) that are allowed for a given set of values of s^2_{23}, $P(\nu_\mu\to\nu_e)$, and $P(\bar{\nu}_\mu\to\bar{\nu}_e)$. Then, we have, in general, four crossing points on the x-y plane for a given value of $\sin^2 2\theta_{23}$, the fourfold degeneracy. Simultaneously, the two $y=$const lines are slightly tilted and the split between the two curves becomes larger at larger $\sin^2 2\theta_{13}$, although the effect is too tiny to be clearly seen. If the baseline distance is longer, the Earth matter effect comes in and further splits each appearance contour into two, depending upon the sign of Δm^2_{31}. Then we have four curves (or two continuous contours, each of which intersects twice with the $y=$const line) and hence there are eight solutions as displayed in Fig. 3.[4] This is a simple pictorial representation of the maximal eightfold parameter degeneracy [24]. To draw Fig. 3, we have calculated disappearance and appearance contours by using the approximate formula derived by Cervera *et al.* [18]. We take the baseline distance and neutrino energy as $L=295$ km and $E=400$ MeV with possible relevance to the JHF project [14]. The Earth matter density is taken to be $\rho=2.3$ g cm^{-3} based on the estimate given in [35]. The electron fraction Y_e is taken to be 0.5. We assume, for definiteness, that a long-baseline disappearance measurement has resulted in $\sin^2 2\theta_{23}=0.92$ and $\Delta m^2_{31}=2.5\times10^{-3}$ eV^2. For the LMA solar neutrino parameters we take $\tan^2\theta_{12}=0.38$ and $\Delta m^2_{21}=6.9\times10^{-5}$ eV^2 [36]. We take the values of these parameters and the matter density throughout this paper unless otherwise stated. The qualitative features of the figure remain unchanged even if we employ values of the parameters obtained by other analyses.

[3]Usually one thinks of determining not $|\Delta m^2_{31}|$ but $|\Delta m^2_{32}|$ by a disappearance measurement. But it does not appear possible to resolve the difference between these two quantities because one has to achieve a resolution of order ϵ for the reconstructed neutrino energy.

[4]The readers might be curious about the feature that the two contours are connected with each other at a large s^2_{23} point. Because δ is a phase variable, the contours must be closed as δ varies.

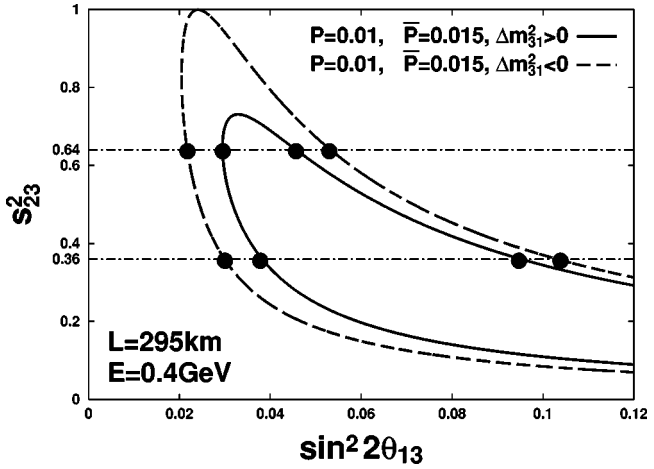

FIG. 3. Depicted in the $\sin^2 2\theta_{13}$-s^2_{23} plane are the contours determined by arbitrarily given values of the appearance probabilities $P \equiv P(\nu_\mu \to \nu_e) = 0.01$ and $\bar{P} \equiv P(\bar{\nu}_\mu \to \bar{\nu}_e) = 0.015$ with E/L off the oscillation maximum ($|\Delta_{31}| \neq \pi$) at the JHF experiment. Here, $s^2_{23} \equiv \sin^2\theta_{23}$. The solid and the dashed lines correspond to positive and negative Δm^2_{31}, respectively. The dash-dotted lines represent the boundary of the region $0.36 \leqslant s^2_{23} \leqslant 0.64$ which is presently allowed by the atmospheric neutrino data, $0.92 \leqslant \sin^2 2\theta_{23} \leqslant 1$. As indicated in the figure, there are four solutions for each s^2_{23}, and altogether there are eight solutions as denoted by blobs for any values of $\theta_{23} \neq \pi/4$. The oscillation parameters are taken as follows: $\Delta m^2_{31} = 2.5 \times 10^{-3}$ eV^2, $\Delta m^2_{21} = 6.9 \times 10^{-5}$ eV^2, $\tan^2\theta_{12} = 0.38$. The Earth density is taken to be $\rho = 2.3$ g/cm^3.

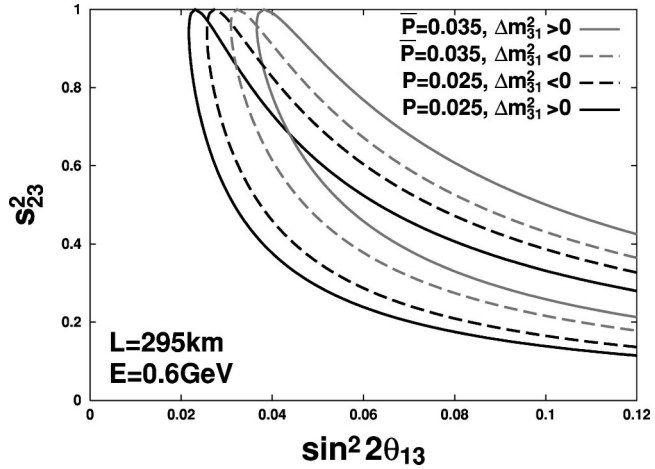

FIG. 4. The allowed regions are shown in the $\sin^2 2\theta_{13}$-s^2_{23} plane determined with a given value of $P \equiv P(\nu_\mu \to \nu_e)$ alone (in this case $P = 0.025$), or $\bar{P} \equiv P(\bar{\nu}_\mu \to \bar{\nu}_e)$ alone (in this case $\bar{P} = 0.035$) at the oscillation maximum $|\Delta_{31}| = \pi$ of the JHF experiment. Each allowed region is the area bounded by the black solid (for $\Delta m^2_{31} > 0$ with P only), the black dashed (for $\Delta m^2_{31} < 0$ with P only), the gray solid (for $\Delta m^2_{31} > 0$ with $\bar{P}$ only), and the gray dashed (for $\Delta m^2_{31} < 0$ with $\bar{P}$ only) line, respectively, where the line with a definite value of the *CP* phase δ sweeps out each region as δ varies from 0 to 2π. The oscillation parameters and the Earth density are the same as those in Fig. 3.

V. RESOLVING THE PARAMETER DEGENERACY BY REACTOR MEASUREMENT OF θ_{13}

Now we discuss how reactor experiments can contribute to resolving the parameter degeneracy. To make our discussion as concrete as possible we use a particular long-baseline experiment, the JHF experiment [14], to illuminate the complementary role played by reactor and long-baseline experiments. It is likely that the experiment will be carried out at around the first oscillation maximum ($|\Delta_{31}| = \pi$) for a number of reasons: the dip in energy spectrum in the disappearance channel is the deepest, the number of appearance events is nearly maximal [14], and the twofold degeneracy in δ becomes simple ($\delta \leftrightarrow \pi - \delta$) for each mass hierarchy [20,24].[5] With the distance $L = 295$ km, the oscillation maximum is at around $E = 600$ MeV. We take the same mixing parameters as those used in Fig. 3.

A. Illustration of how reactor measurement helps resolve the (θ_{13}, θ_{23}) degeneracy

Let us first give an illustrative example showing how reactor experiments could help resolve the (θ_{13}, θ_{23}) degeneracy. To present a clear step-by-step explanation of the relationship between LBL and reactor experiments, we first plot in Fig. 4 the allowed regions in the $\sin^2 2\theta_{13}$-s^2_{23} plane by separate measurements of $P(\nu_\mu \to \nu_e)$ alone and $P(\bar{\nu}_\mu \to \bar{\nu}_e)$ alone. The former are indicated by the regions bounded by black lines and the latter by gray lines. The solid and dashed lines are used for cases with positive and negative Δm^2_{31}. The values of disappearance and appearance probabilities are chosen arbitrarily for illustrative purposes and are given in the caption of Fig. 4. Notice that the negative Δm^2_{31} curve is located right (left) of the positive Δm^2_{31} curve in the neutrino (antineutrino) channel. The plot with measurements in only the neutrino mode has more than academic interest because the JHF experiment is expected to run only with the neutrino mode in its first phase. We observe that there is large intrinsic uncertainty in the θ_{13} determination due to the unknown δ, the problem addressed in [20]. The two regions corresponding to positive and negative Δm^2_{31} heavily overlap due to the small matter effect. When two measurements of the ν and $\bar{\nu}$ channels are combined, the allowed solution becomes a line which lies inside the overlap of the ν and $\bar{\nu}$ regions for each sign of Δm^2_{31} in Fig. 4.[6] In Fig. 5 we have plotted such solutions as two lines, one for

[5] In order to have this reduction, one has to actually tune the energy spectrum so that the $\cos\delta$ term in Eq. (10) averaged over the energy with the neutrino flux times the cross section vanishes, which is shown to be possible in [20].

[6] In the absence of the matter effect, the reason why the closed curve shrinks to a line at the oscillation maximum can be seen as follows. By eliminating δ in Eq. (10), it is easy to show that there are two solutions of $\sin 2\theta_{13} > 0$ for given values of P, $\bar{P}$, and θ_{23} off the oscillation maximum ($\Delta_{31} \neq \pi$), whereas there is only one solution of $\sin 2\theta_{13} > 0$ at the oscillation maximum ($\Delta_{31} = \pi$). Even if we switch on the matter effect, one can easily show by using the approximate formula in [18] that the same argument holds.

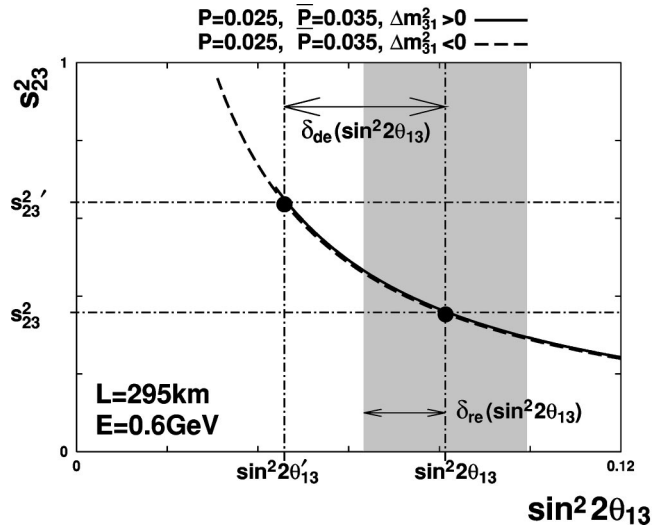

FIG. 5. The allowed region in the $\sin^2 2\theta_{13}$-s^2_{23} plane becomes a line when both $P(\nu_\mu \to \nu_e)$ and $P(\bar{\nu}_\mu \to \bar{\nu}_e)$ are given [in this case $P(\nu_\mu \to \nu_e)=0.025$, $P(\bar{\nu}_\mu \to \bar{\nu}_e)=0.035$] at the oscillation maximum ($|\Delta_{31}|=\pi$, $E=0.6$ GeV for the JHF experiment), as indicated in the figure. The solid and the dashed lines are for the $\Delta m^2_{31}>0$ and $\Delta m^2_{31}<0$ cases, respectively. Assuming $\theta_{23} \neq \pi/4$, two solutions of $(\sin^2 2\theta_{13}, s^2_{23})$ are plotted; in this figure $\sin^2 2\theta_{23}$ is taken as 0.92. It is assumed arbitrarily that the solution of θ_{23} in the first octant ($\theta_{23}<\pi/4$) is the genuine one, while the one in the second octant ($\theta_{23}>\pi/4$) with primes is the fake one. Superimposed in the figure as a shaded region is the anticipated error in the reactor measurement of θ_{13} estimated in Sec. III. If the error $\delta_{re}(\sin^2 2\theta_{13})$ is smaller than the difference $\delta_{de}(\sin^2 2\theta_{13}) \equiv |\sin^2 2\theta'_{13} - \sin^2 2\theta_{13}|$ due to the degeneracy, then the reactor experiment may be able to resolve it.

positive Δm^2_{31} (the solid curve) and the other for negative Δm^2_{31} (the dashed curve) at the first oscillation maximum $|\Delta_{31}|=\pi$. It may appear curious that the two curves with positive and negative Δm^2_{31} almost overlap with each other in Fig. 5. In fact, the slight split between the solid ($\Delta m^2_{31}>0$) and dashed ($\Delta m^2_{31}<0$) lines is due to the fact that both ϵ and the matter effect in the case of the JHF experiment are small. Thus, the degeneracy in the set $(\theta_{13}, \theta_{23})$ is effectively twofold in this case.

To get a feeling as to whether the reactor experiment described in Sec. III will be able to resolve the degeneracy, we plot in Fig. 5 two sets of degenerate solutions by taking a particular value of θ_{23}, $\sin^2 2\theta_{23}=0.92$, the lower end of the region allowed by Super-Kamiokande. We denote the true and fake solutions as $(\sin^2 2\theta_{13}, s^2_{23})$ and $(\sin^2 2\theta'_{13}, s^2_{23}{}')$, respectively, assuming that the true θ_{23} satisfies $\theta_{23}<\pi/4$. We overlay in Fig. 5 a shadowed region to indicate the accuracy to be achieved by the reactor measurement of θ_{13}. If the experimental error $\delta_{re}(\sin^2 2\theta_{13})$ in the reactor measurement of $\sin^2 2\theta_{13}$ is smaller than the difference

$$\delta_{de}(\sin^2 2\theta_{13}) \equiv |\sin^2 2\theta'_{13} - \sin^2 2\theta_{13}| \tag{11}$$

due to the $(\theta_{13}, \theta_{23})$ degeneracy, then the reactor experiment may resolve the degeneracy. Notice that once the θ_{23} degeneracy is lifted one can easily obtain four allowed sets of $(\delta, \Delta m^2_{31})$ (although they are still degenerate at almost the same point on the $\sin^2 2\theta_{13}$-s^2_{23} plane) because the relationship between them has been given analytically in a completely general setting [26].

B. Resolving power of the $(\theta_{13}, \theta_{23})$ degeneracy by a reactor measurement

Let us make a semiquantitative estimate of how powerful the reactor method is for resolving the $(\theta_{13}, \theta_{23})$ degeneracy.[7] For this purpose, we compare in this section the difference of the two θ_{13} solutions due to the degeneracy with the resolving power of the reactor experiment. We consider, for simplicity, the special case $|\Delta_{31}|=\pi$, i.e., energy tuned at the first oscillation maximum. The simplest case seems to be indicative of features of more generic cases.

As we saw in the previous section, there are two solutions of θ_{13} due to the doubling of θ_{23} for a given $\sin^2 2\theta_{23}$ for in each sign of Δm^2_{31}. Then we define the fractional difference due to the degeneracy

$$\frac{\delta_{de}(\sin^2 2\theta_{13})}{\sin^2 2\theta_{13}}. \tag{12}$$

It is to be compared with $\delta_{re}(\sin^2 2\theta_{13})/\sin^2 2\theta_{13}$ of the reactor experiment, where $\delta_{re}(\sin^2 2\theta_{13})$ denotes the experimental uncertainty estimated in Sec. III, i.e., 0.043 or 0.018. In Fig. 6(a) we plot the normalized error $\delta_{re}(\sin^2 2\theta_{13})/\sin^2 2\theta_{13}$ which is expected to be achieved in the reactor experiment described in Sec. III. We restrict ourselves to an analysis with one degree of freedom, because we expect that the JHF phase I experiment will provide us with accurate information on Δm^2_{31} by the time the issue is really focused on the degeneracy in JHF phase II. The fractional difference (12) can be computed from the relation [24]

$$\sin^2 2\theta'_{13} = \sin^2 2\theta_{13} \tan^2 \theta_{23} + \left(\frac{\Delta m^2_{21}}{\Delta m^2_{31}}\right)^2 \frac{\tan^2(aL/2)}{(aL/\pi)^2} \times [1-(aL/\pi)^2] \sin^2 2\theta_{12} (1-\tan^2\theta_{23}), \tag{13}$$

and the result for $\delta_{de}(\sin^2 2\theta_{13})/\sin^2 2\theta_{13}$ is plotted in Fig. 6(b) as a function of $\sin^2 \theta_{23}$ for two typical values of ϵ. We notice that the fractional differences differ by up to a factor of ~ 2 in the small $\sin^2 2\theta_{23}$ region between the first ($\theta_{23}<\pi/4$) and the second octants ($\theta_{23}>\pi/4$). For the best fit value of the two mass squared differences Δm^2_{21} (6.9×10^{-5} eV^2) and $|\Delta m^2_{31}|$ (2.5×10^{-3} eV^2), for which $\epsilon \equiv \Delta m^2_{21}/|\Delta m^2_{31}|=0.028$, there is little difference between the case with $\sin^2 2\theta_{13}=0.03$ and the one with $\sin^2 2\theta_{13}=0.09$. In

[7]The possibility of resolving the $(\theta_{13}, \theta_{23})$ by a reactor experiment was qualitatively mentioned in [21,34]. An alternative way to resolve the ambiguity is to look at the $\nu_e \to \nu_\tau$ channel because the main oscillation term in the probability $P(\nu_e \to \nu_\tau)$ depends upon c^2_{13}. Unfortunately, this idea does not appear to have been explored in detail, although it is briefly mentioned in [24,25].

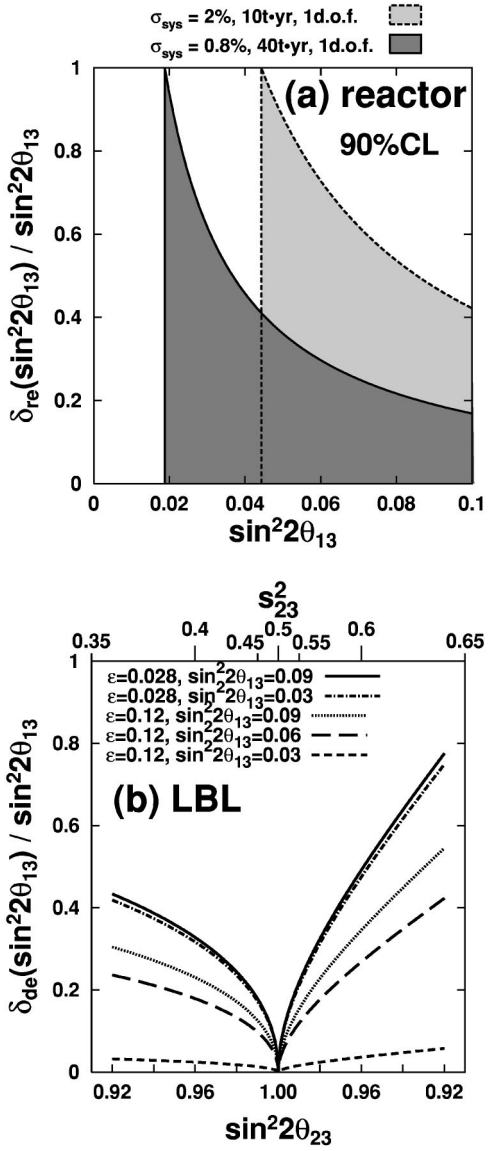

FIG. 6. (a) The normalized error at 90% C.L. in the reactor measurement of θ_{13} is given for $\sigma_{\rm sys}=2\%$, 10 ton yr [DOF$=1$, $\delta_{\rm re}(\sin^2 2\theta_{13})=0.043$] in gray and for $\sigma_{\rm sys}=0.8\%$, 40 ton yr [DOF$=1$, $\delta_{\rm re}(\sin^2 2\theta_{13})=0.018$] in black, respectively. Notice that the number of degrees of freedom becomes 1 once the value of $|\Delta m^2_{31}|$ is known from JHF. (b) The fractional difference $\delta_{\rm de}(\sin^2 2\theta_{13})/\sin^2 2\theta_{13}$ due to the degeneracy is plotted as a function of $\sin^2 2\theta_{23}$. Here, $\delta_{\rm de}(\sin^2 2\theta_{13})\equiv|\sin^2 2\theta'_{13}-\sin^2 2\theta_{13}|$ stands for the difference between the true solution $\sin^2 2\theta_{13}$ and the fake one $\sin^2 2\theta'_{13}$, and $\epsilon\equiv\Delta m^2_{21}/|\Delta m^2_{31}|$; $\epsilon=6.9\times10^{-5}$ eV^2/2.5 $\times10^{-3}$ eV$^2=0.028$ is for the best fit, and an extreme case with $\epsilon=1.9\times10^{-4}$ eV^2/1.6$\times10^{-3}$ eV$^2=0.12$, which is allowed at 90% C.L. (atmospheric) or 95% C.L. (solar), is also shown for illustration. The horizontal axis is suitably defined so that it is linear in $\sin^2 2\theta_{23}$, where the left half is for $\theta_{23}<\pi/4$ whereas the right half is for $\theta_{23}>\pi/4$. The solar mixing angle is taken as $\tan^2\theta_{12}=0.38$. $\sin^2 2\theta_{23}\geqslant 0.92$ has to be satisfied due to the constraint from the super-Kamiokande atmospheric neutrino data. If the value of $\cos^2 2\theta_{23}$ is large enough, the value of $\delta_{\rm de}(\sin^2 2\theta_{13})/\sin^2 2\theta_{13}$ increases and lies outside the normalized error of the reactor experiment; then the reactor result may resolve the θ_{23} ambiguity.

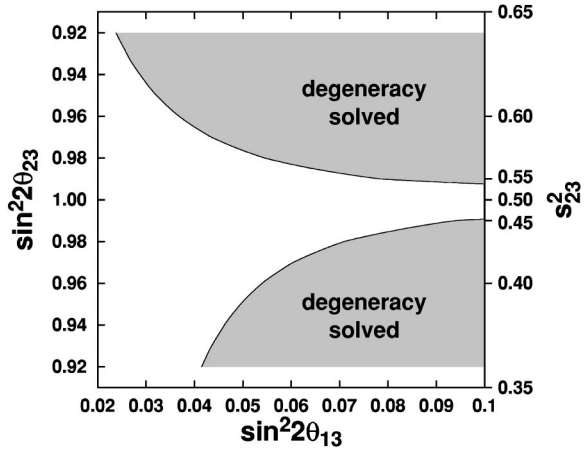

FIG. 7. The shadowed area stands for the region in which $\delta_{\rm re}(\sin^2 2\theta_{13})<\delta_{\rm de}(\sin^2 2\theta_{13})$ is satisfied for $\sigma_{\rm sys}=0.8\%$, 40 ton yr, DOF$=1$, and for the best fit values of the solar and atmospheric oscillation parameters. In this shadowed region, the $(\theta_{13},\theta_{23})$ degeneracy may be solved. The vertical axis is the same as the horizontal axis of Fig. 6(b).

this case they are all approximated by the first term in Eq. (13), and $\delta_{\rm de}(\sin^2 2\theta_{13})/\sin^2 2\theta_{13}$ depends approximately only on θ_{23}, making the analysis easier. On the other hand, if the ratio $\epsilon\equiv\Delta m^2_{21}/|\Delta m^2_{31}|$ is much larger than that at the best fit point, then the second term in Eq. (13) is not negligible. In Fig. 6(b), $\delta_{\rm de}(\sin^2 2\theta_{13})/\sin^2 2\theta_{13}$ is plotted in the extreme case of $\epsilon=1.9\times10^{-4}$ eV^2/1.6$\times10^{-3}$ eV$^2=0.12$, which is allowed at the 90% C.L. (atmospheric) or the 95% C.L. (solar), with $\sin^2 2\theta_{13}=0.03$, 0.06, 0.09. From this, we observe that the suppression in the first term in Eq. (13) is compensated by the second term for $\sin^2 2\theta_{13}=0.03$, i.e., the degeneracy is small and therefore resolving the degeneracy is difficult in this case. To clearly illustrate the resolving power of the degeneracy in the reactor measurement, assuming the best fit value $\epsilon=0.028$, we plot in Fig. 7 the region where the degeneracy can be lifted in the $\sin^2 2\theta_{13}$-$\sin^2 2\theta_{23}$ plane. It is evident that the reactor measurement will be able to resolve the $(\theta_{13},\theta_{23})$ degeneracy in a wide range inside its sensitivity region, in particular for θ_{23} in the second octant.

A quantitative estimation of the significance of the fake solution requires a detailed analysis of accelerator experiments which includes the statistical and systematic errors as well as the correlations of errors and the parameter degeneracies, and it will be worked out in future research.

VI. MORE ABOUT REACTOR VS LONG-BASELINE EXPERIMENTS

The discussions in the previous section implicitly assume that the sensitivities of the reactor and LBL experiments with both ν and $\bar{\nu}$ channels are good enough to detect the effects of nonzero θ_{13}. However, this need not be true, in particular, in the coming decade. To further illuminate the complementary roles played by reactor and LBL experiments, we examine their possible mutual relationship, including the cases where there is a signal in the former but none in the latter

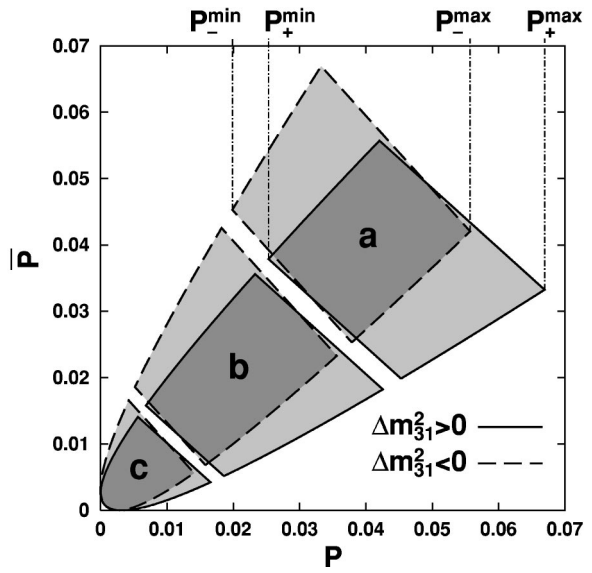

FIG. 8. Predicted allowed regions are depicted in the P-$\bar{P}$ plane for the JHF experiment at the oscillation maximum after an affirmative (a negative) result of the reactor experiment is obtained, where $P \equiv P(\nu_\mu \to \nu_e)$ and $\bar{P} \equiv P(\bar{\nu}_\mu \to \bar{\nu}_e)$ are the appearance probabilities, and $\theta_{23} = \pi/4$ is assumed. The cases a, b, and c correspond to $\sin^2 2\theta_{13} = 0.08 \pm 0.018$, $\sin^2 2\theta_{13} = 0.04 \pm 0.018$, and $\sin^2 2\theta_{13} < 0.019$, respectively. The regions bounded by the solid lines and the dashed lines are for the normal hierarchy ($\Delta m^2_{31} > 0$) and the inverted hierarchy ($\Delta m^2_{31} < 0$), respectively. Each region predicts the maximum ($P_\pm^{\max}$) and the minimum ($P_\pm^{\min}$) values of P for each hierarchy ($+$ for the normal and $-$ for the inverted hierarchy), although $P_\pm^{\min}$ of the region c are zero.

experiments, or vice versa. For ease of understanding by the readers, we restrict our presentation in this section to a very intuitive level by using a figure. It is, of course, possible to make it more precise by deriving inequalities based on the analytical approximate formulas [18]. Throughout this section LBL experiments at the oscillation maximum and $\theta_{23} = \pi/4$ are assumed.

If a reactor experiment sees affirmative evidence for the disappearance in $\bar{\nu}_e \to \bar{\nu}_e$ (the case of reactor affirmative), it will be possible to determine θ_{13} up to certain experimental errors. In this case, the appearance probability in LBL experiment must fall into the region $P(\nu)_\pm^{\min} \leqslant P(\nu) \leqslant P(\nu)_\pm^{\max}$ if the mass hierarchy is known, where the $+$ $(-)$ sign refers to $\Delta m^2_{31} > 0$ ($\Delta m^2_{31} < 0$) and max (min) refers to the maximum (minimum) value of the allowed region for $P \equiv P(\nu_\mu \to \nu_e)$, respectively. (See Fig. 8.) Without knowledge of the mass hierarchy, the probability is within the region $P(\nu)_-^{\min} \leqslant P(\nu) \leqslant P(\nu)_+^{\max}$. Similar inequalities are present also for the antineutrino appearance channel. In Fig. 8 we present the allowed regions in the cases of $\Delta m^2_{31} > 0$ and $\Delta m^2_{31} < 0$ on a plane spanned by $P(\nu_\mu \to \nu_e)$ and $P(\bar{\nu}_\mu \to \bar{\nu}_e)$ by taking the two best fit values $\sin^2 2\theta_{13} = 0.08$ and 0.04 (labeled as a and b) as reactor affirmative cases. They are inside the sensitivity region of the reactor experiment discussed in Sec. III. We have used a one-dimensional χ^2 analysis (i.e., the only parameter is $\sin^2 2\theta_{13}$) to obtain the allowed regions in Fig. 8. In doing this we have used the same systematic error of 0.8% and the statistical errors corresponding to 40 ton yr measurement by the detector considered in Sec. III. For $\sin^2 2\theta_{13} \lesssim 0.02$, this particular reactor experiment would fail (the case of reactor negative) but the allowed region can be obtained by the same procedure, and is presented in Fig. 8, the region labeled as c. We use the same LMA parameters as used earlier for Fig. 3 and Fig. 4.

We discuss four cases depending upon the two possibilities of affirmative and negative evidence in each disappearance and appearance search in the reactor and long-baseline accelerator experiments. However, it is convenient to organize our discussion by classifying the possibilities into two categories, reactor affirmative and reactor negative.

A. Reactor affirmative

We have two alternative cases, the LBL appearance search affirmative or negative.

1. LBL affirmative

The implications of affirmative evidence in the appearance search in LBL experiments differ depending upon the region in which the observed appearance probability $P(\nu)$ falls.

(1) $P_-^{\min} \leqslant P(\nu) \leqslant P_+^{\min}$ or

(2) $P_-^{\max} \leqslant P(\nu) \leqslant P_+^{\max}$. These cases correspond to the two intervals that are given by the projection on the P axis of the whole shadowed region (a or b) minus the projection on the P axis of the darker shadowed region (a or b) in Fig. 8. It is remarkable that in these cases not only is the sign of Δm^2_{31} determined, but also the CP phase δ is known to be nonvanishing. If $P(\nu)$ is in the former region then Δm^2_{31} is negative and $\sin\delta$ is positive, whereas if $P(\nu)$ is in the latter then Δm^2_{31} is positive and $\sin\delta$ is negative.

(3) $P_+^{\min} \leqslant P(\nu) \leqslant P_-^{\max}$. This case corresponds to the interval that is given by the projection on the P axis of the darker shadowed region (a or b) in Fig. 8. In this case, neither the sign of Δm^2_{31} nor the sign of $\sin\delta$ can be determined.

It may be worth noting that if the reactor determination of θ_{13} is accurate enough, it could be advantageous for LBL appearance experiments to run only in the neutrino mode (where the cross section is larger than that for antineutrinos by a factor of 2–3) to possibly determine the sign of Δm^2_{31} depending upon the region in which $P(\nu)$ falls.

2. LBL negative

In principle, it is possible to have no appearance event even though the reactor sees evidence for disappearance. This case corresponds to the left edge of the analogous shadowed region in the case of $\sin^2 2\theta_{13} \simeq 0.02$ in Fig. 8, i.e., the allowed region with $\sin^2 2\theta_{13} \simeq 0.02$ for which $P_-^{\min}$ on the P axis falls below $P = 0.005$. In order for this case to occur the sensitivity limits $P(\nu)_{\rm limit}$ of the LBL experiment must satisfy $P_-^{\min} < P(\nu)_{\rm limit}$, assuming our ignorance of the sign of Δm^2_{31}. If it occurs that $P_-^{\min} < P(\nu)_{\rm limit} < P_+^{\min}$, then the sign of Δm^2_{31} is determined to be minus.

The $P(\nu)_{\rm limit}$ of the JHF experiment in its phase I is estimated to be 3×10^{-3} [14].[8] Therefore, by using the mixing parameters typical for the LMA solution, the case of LBL negative cannot occur unless the sensitivity of the reactor experiment becomes $\sin^2 2\theta_{13} \lesssim 0.01$. However, in the intermediate stage of the JHF experiment, where $P(\nu)_{\rm limit}$ is larger than 3×10^{-3}, this situation may occur.

B. Reactor negative

If the reactor experiment does not see disappearance of $\overline{\nu}_e$ one obtains the bound $\theta_{13} \leqslant \theta_{13}^{\rm RL}$. We have again two alternative cases, the LBL appearance search affirmative or negative.

1. LBL affirmative

If a LBL experiment measures the oscillation probability $P(\nu)$, then, for a given value of $P(\nu)$ the allowed region of $\sin 2\theta_{13}$ is given by $\sin 2\theta_{\pm}^{\rm min} \leqslant \sin 2\theta_{13} \leqslant \sin 2\theta_{\pm}^{\rm max}$ if the sign of Δm^2_{31} is known, and by $\sin 2\theta_{+}^{\rm min} \leqslant \sin 2\theta_{13} \leqslant \sin 2\theta_{-}^{\rm max}$ otherwise. We denote below the maximum and the minimum values of θ_{13} collectively as $\theta_{\rm max}$ and $\theta_{\rm min}$, respectively. In Fig. 4, the region bounded by $\sin 2\theta_{+}^{\rm min}$ and $\sin 2\theta_{+}^{\rm max}$ ($\sin 2\theta_{-}^{\rm min}$ and $\sin 2\theta_{-}^{\rm max}$) is indicated as the region bounded by the solid (dashed) black line for a given value of s^2_{23}.

Then, there are two possibilities which we discuss one by one.

(i) $\theta_{13}^{\rm RL} \geqslant \theta_{\rm max}$: In this case no additional information is obtained by nonobservation of disappearance of $\overline{\nu}_e$ in the reactor experiment.

(ii) $\theta_{\rm min} \leqslant \theta_{13}^{\rm RL} \leqslant \theta_{\rm max}$: In this case we have the nontrivial constraint $\theta_{\rm min} \leqslant \theta_{13} \leqslant \theta_{13}^{\rm RL}$.

2. LBL negative

In this case, we obtain an upper bound on θ_{13}, which, however, depends on the assumed values of δ and the sign of Δm^2_{31}. A δ-independent bound can also be derived: $\theta_{13} \leqslant \min[\theta_{13}^{\rm RL}, \theta_{\rm max}]$.

[8]The sensitivity limit of $\sin^2 2\theta_{13}$ quoted in [14], $\sin^2 2\theta_{13} \leqslant 6\times10^{-3}$, obtained by using the one-mass-scale approximation ($\epsilon \ll 1$), may be translated into this limit for $P(\nu)$.

VII. DISCUSSION AND CONCLUSION

In this paper, we have explored in detail the possibility of measuring $\sin^2 2\theta_{13}$ using reactor neutrinos. We stressed that this measurement is free from the problem of parameter degeneracies from which accelerator appearance experiments suffer, and that the reactor measurement is complementary to accelerator experiments. We showed that sensitivity to $\sin^2 2\theta_{13} \gtrsim 0.02$ (0.05) is obtained with a 24.3 $\rm GW_{th}$ reactor with identical detectors at near and far distances and with a data size of 40 (10) ton yr, assuming that the relative systematic error is 0.8% (2%) for the total number of events. In particular, if the relative systematic error is 0.8%, the error in $\sin^2 2\theta_{13}$ is 0.018, which is smaller than the uncertainty due to the combined (intrinsic and hierarchical) parameter degeneracies expected in accelerator experiments. We also showed that the reactor measurement can resolve the degeneracy in $\theta_{23} \leftrightarrow \pi/2 - \theta_{23}$ and determine whether θ_{23} is smaller or larger than $\pi/4$ if $\sin^2 2\theta_{13}$ and $\cos^2 2\theta_{23}$ are relatively large.

We took 2% and 0.8% as the reference values for the relative systematic error for the total number of events. 2% is exactly the same figure as in the Bugey experiment while 0.8% is what we naively expect in the case where we have two identical detectors, near and far, which are similar to that of the CHOOZ experiment. It is also technically possible to dig a 200 m depth shaft hole with diameter wide enough to place a CHOOZ-like detector in. Therefore, the discussions in this paper are realistic. We hope the present paper stimulates the interest of the community in reactor measurements of θ_{13}.

ACKNOWLEDGMENTS

We thank Yoshihisa Obayashi for correspondence and Michael Shaevitz for useful comments. H.M. thanks Andre de Gouvea for discussions and the Theoretical Physics Department of Fermilab for hospitality. H.S. acknowledges the hospitality of Professor Atsuto Suzuki and the members of the Research Center for Neutrino Science, Tohoku University, where a core part of the sensitivity analysis was carried out. This work was supported by Grants-in-Aid for Scientific Research in Priority Areas No. 12047222 and No. 13640295, Japan Ministry of Education, Culture, Sports, Science, and Technology.

[1] Kamiokande Collaboration, Y. Fukuda *et al.*, Phys. Lett. B **335**, 237 (1994); Super-Kamiokande Collaboration, Y. Fukuda *et al.*, Phys. Rev. Lett. **81**, 1562 (1998); Super-Kamiokande Collaboration, S. Fukuda *et al.*, *ibid.* **85**, 3999 (2000).

[2] B.T. Cleveland *et al.*, Astrophys. J. **496**, 505 (1998); SAGE Collaboration, J.N. Abdurashitov *et al.*, Phys. Rev. C **60**, 055801 (1999); GALLEX Collaboration, W. Hampel *et al.*, Phys. Lett. B **447**, 127 (1999); Super-Kamiokande Collaboration, S. Fukuda *et al.*, Phys. Rev. Lett. **86**, 5651 (2001); **86**, 5656 (2001); SNO Collaboration, Q.R. Ahmad *et al.*, *ibid.* **87**, 071301 (2001); **89**, 011301 (2002).

[3] SNO Collaboration, Q.R. Ahmad *et al.*, Phys. Rev. Lett. **89**, 011302 (2002).

[4] K2K Collaboration, S.H. Ahn *et al.*, Phys. Lett. B **511**, 178 (2001); Super-Kamiokande and K2K Collaborations, T. Nakaya, hep-ex/0209036; K. Nishikawa, Nucl. Phys. B (Proc. Suppl.) **118**, 129 (2003).

[5] Z. Maki, M. Nakagawa, and S. Sakata, Prog. Theor. Phys. **28**, 870 (1962).

[6] CHOOZ Collaboration, M. Apollonio *et al.*, Phys. Lett. B **420**,

397 (1998); **466**, 415 (1999).
[7] J. Shirai, Nucl. Phys. B (Proc. Suppl.) **118**, 15 (2003).
[8] L. Wolfenstein, Phys. Rev. D **17**, 2369 (1978).
[9] S.P. Mikheyev and A.Yu. Smirnov, Yad. Fiz. **42**, 1441 (1985) [Sov. J. Nucl. Phys. **42**, 913 (1985)]; Nuovo Cimento Soc. Ital. Fis., C **9**, 17 (1986).
[10] M.B. Smy, in *Neutrino Oscillations and Their Origin*, Kashiwa, 2001, edited by Y. Suzuki *et al.* (World Scientific, Singapore, 2003), p. 40, hep-ex/0202020; J.N. Bahcall, M.C. Gonzalez-Garcia, and C. Pena-Garay, J. High Energy Phys. **07**, 054 (2002); V. Barger, D. Marfatia, K. Whisnant, and B.P. Wood, Phys. Lett. B **537**, 179 (2002); A. Bandyopadhyay, S. Choubey, S. Goswami, and D.P. Roy, *ibid.* **540**, 14 (2002); P.C. de Holanda and A.Y. Smirnov, Phys. Rev. D **66**, 113005 (2002); G.L. Fogli, E. Lisi, A. Marrone, D. Montanino, and A. Palazzo, *ibid.* **66**, 053010 (2002); M. Maltoni, T. Schwetz, M.A. Tortola, and J.W. Valle, *ibid.* **67**, 013011 (2003).
[11] Y. Kozlov, L. Mikaelyan, and V. Sinev, Yad. Fiz. **66**, 497 (2003) [Phys. At. Nucl. **66**, 469 (2003)].
[12] MINOS Collaboration, P. Adamson *et al.*, ''MINOS Detectors Technical Design Report, Version 1.0,'' Report No. NuMI-L-337, 1998, http://www.hep.anl.gov/ndk/hypertext/minos_tdr.html
[13] M. Komatsu, P. Migliozzi, and F. Terranova, J. Phys. G **29**, 443 (2003).
[14] Y. Itow *et al.*, hep-ex/0106019.
[15] H. Minakata and H. Nunokawa, Phys. Lett. B **495**, 369 (2000); Nucl. Instrum. Methods Phys. Res. A **472**, 421 (2000); J. Sato, *ibid.* **472**, 434 (2000); B. Richter, hep-ph/0008222.
[16] CERN Working Group on Super Beams Collaboration, J.J. Gomez-Cadenas *et al.*, hep-ph/0105297.
[17] D. Ayres *et al.*, hep-ex/0210005.
[18] A. Cervera, A. Donini, M.B. Gavela, J.J. Gomez Cadenas, P. Hernandez, O. Mena, and S. Rigolin, Nucl. Phys. **B579**, 17 (2000); **B593**, 731(E) (2001).
[19] C. Albright *et al.*, hep-ex/0008064; V.D. Barger, S. Geer, R. Raja, and K. Whisnant, Phys. Rev. D **63**, 113011 (2001); J. Pinney and O. Yasuda, *ibid.* **64**, 093008 (2001); P. Hernandez and O. Yasuda, Nucl. Instrum. Methods Phys. Res. A **485**, 811 (2002); O. Yasuda, *ibid.* **503**, 104 (2003); in *Neutrino Oscillations and Their Origin* [10], p. 259, hep-ph/0203273; hep-ph/0209127, and references therein.
[20] T. Kajita, H. Minakata, and H. Nunokawa, Phys. Lett. B **528**, 245 (2002).
[21] G. Fogli and E. Lisi, Phys. Rev. D **54**, 3667 (1996).
[22] J. Burguet-Castell, M.B. Gavela, J.J. Gomez-Cadenas, P. Hernandez, and O. Mena, Nucl. Phys. **B608**, 301 (2001).
[23] H. Minakata and H. Nunokawa, J. High Energy Phys. **10**, 001 (2001); Nucl. Phys. B (Proc. Suppl.) **110**, 404 (2002).
[24] V. Barger, D. Marfatia, and K. Whisnant, Phys. Rev. D **65**, 073023 (2002); in Proceedings of the APS/DPF/DPB Summer Study on the Future of Particle Physics, Snowmass, 2001, edited by R. Davidson and C. Quigg, hep-ph/0108090.
[25] A. Donini, D. Meloni, and P. Migliozzi, Nucl. Phys. **B646**, 321 (2002).
[26] H. Minakata, H. Nunokawa, and S. Parke, Phys. Rev. D **66**, 093012 (2002).
[27] Particle Data Group, K. Hagiwara *et al.*, Phys. Rev. D **66**, 010001 (2002).
[28] T.K. Kuo and J. Pantaleone, Phys. Lett. B **198**, 406 (1987); H. Minakata and S. Watanabe, *ibid.* **468**, 256 (1999). In a recent paper, a similar treatment is generalized into all other channels; H. Yokomakura, K. Kimura, and A. Takamura, *ibid.* **544**, 286 (2002).
[29] M. Shiozawa, talk presented at XXth International Conference on Neutrino Physics and Astrophysics, Neutrino 2002, Munich, Germany.
[30] M.C. Gonzalez-Garcia and C. Pena-Garay, Phys. Lett. B **527**, 199 (2002).
[31] Y. Declais *et al.*, Nucl. Phys. **B434**, 503 (1995).
[32] G.L. Fogli and E. Lisi, Phys. Rev. D **52**, 2775 (1995).
[33] J. Arafune, M. Koike, and J. Sato, Phys. Rev. D **56**, 3093 (1997); **60**, 119905(E) (1999).
[34] G. Barenboim and A. de Gouvea, hep-ph/0209117.
[35] M. Koike and J. Sato, Mod. Phys. Lett. A **14**, 1297 (1999).
[36] Super-Kamiokande Collaboration, S. Fukuda *et al.*, Phys. Lett. B **539**, 179 (2002).